Particles and the Cosmos

2019/2020

Sascha Caron, Jörg Hörandel

NM109
first semester, 6 ec

32 hrs lecture Wednesday 10:30 - 12:15 HG 00.086
32 hrs problem session Thursday 13:30 - 15:15 HG 02.052

Exam:
Written exam.

Lectures:

Experimental methods (JRH)
04.09.2019 1. Interactions with matter
11.09.2019 2. Detectors
Standard model (SC)
18.09.2019 3. Particles, QED, Feynman rules
25.09.2019 4. Hadrons and QCD
02.10.2019 5. Hadrons and QCD
09.10.2019 6. Weak interactions, CP violation
16.10.2019 7. Higgs mechanism
Astroparticle physics (JRH)
06.11.2019 8. The birth of cosmic rays
13.11.2019 9. Cosmic rays in the Galaxy, in the heliosphere, and the Earth magnetic field
20.11.2019 10. Cosmic rays at the top of and in the atmosphere
27.11.2019 11. Cosmic rays underground - neutrino oscillations
04.12.2019 12. Neutrino oscillations, Astroparticle Physics
Beyond the Standard Model, Dark Matter (SC)
11.12.2019 13. Lambda CDM, Big-bang nucleosynthesis
18.12.2019 14. Dark matter - Beyond-the-standard-model reasons

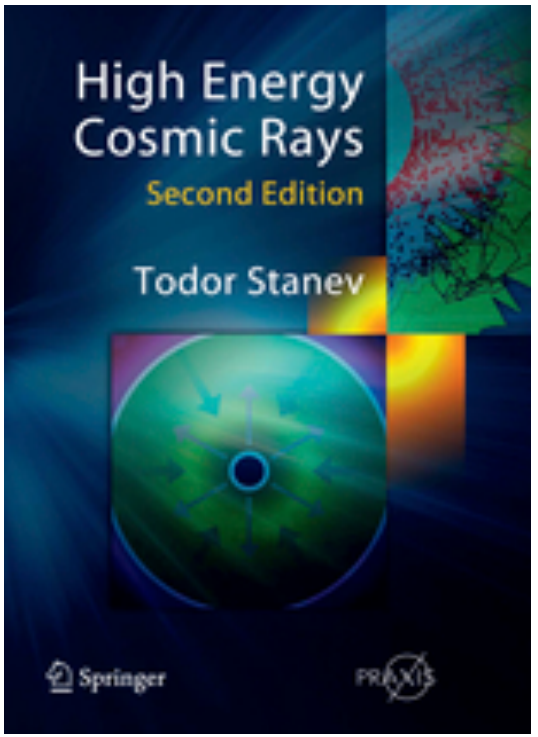

Jörg R. Hörandel
HG 02.721
http://particle.astro.ru.nl

Interactions of particles with matter

electromagnetic processes

- Coulomb scattering
- ionization loss
- Cherenkov light
- bremsstrahlung

photon interactions

- photo effect
- Compton scattering
- pair production

e/m collisions on magnetic and photon fields

- synchrotron radiation
- inverse Compton effect

hadronic interactions

- secondary particles, multiplicity, inelasticity
- nuclear fragmentation

http://pdg.lbl.gov

PDG particle data group 1957 2017 Reviews, Tables and Plots

HOME: | pdgLive | Summary Tables | Reviews, Tables, Plots | Particle Listings

2018 Review of Particle Physics

Please use this **CITATION**:
M. Tanabashi *et al.* (Particle Data Group), Phys. Rev. D **98**, 030001 (2018).

Downloadable figures are available for these reviews.

Reviews, Tables & Plots

Search Reviews

Categories:

Close/Open categories

- **Introduction, History plots, Online information**
- **Constants, Units, Atomic and Nuclear Properties**
- **Standard Model and Related Topics**
- **Astrophysics and Cosmology**
- **Experimental Methods and Colliders**
- **Mathematical Tools**
- **Kinematics, Cross-Section Formulae, and Plots**
- **Particle Properties**
  (Hypothetical particles are in a different section further below.)
- **Hypothetical Particles and Concepts**

Experimental Methods and Colliders

- Accelerator physics of colliders (rev.)
- High-energy collider parameters (rev.)
- Neutrino beam lines at High-energy proton synchrotrons (rev.
- Passage of particles through matter
- Particle detectors at accelerators (rev.)
- Particle detectors for non-accelerator physics (rev.)
- Radioactivity and radiation protection (rev.)
- Commonly used radioactive sources (rev.)

Coulomb scattering

the basis of all electromagnetic interactions is the Coulomb scattering between two electric charges $F = \frac{q_1 q_2}{R^2}$

deflection angle $\tan\frac{\theta}{2} = \frac{zZe^2}{Mv^2 b}$ b **impact parameter**

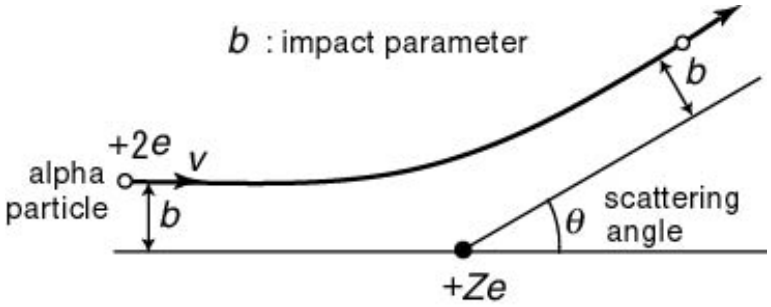

differential cross section for electron scattering (*z=1*)

$$\frac{d\sigma}{d\Omega} = \frac{b}{\sin\theta}\frac{db}{d\theta} = \frac{Z^2}{4} r_e^2 \sin^{-4}\frac{\theta}{2}$$

Z **charge of medium**

classical electron radius $r_e = \frac{e^2}{m_e c^2}$

momentum transfer

$$q = 2p\sin\frac{\theta}{2}$$

p **electron momentum before scattering**

Ionization loss

charged particles traveling through matter lose energy on excitation and ionization of its atoms

energy loss per unit of column depth [MeV per g/cm²]

Bethe-Bloch equation

$$\frac{dE}{dx} = -\frac{N_A Z}{A}\frac{2\pi(ze^2)^2}{Mv^2}\left[\ln\frac{2Mv^2\gamma^2 W}{I^2} - 2\beta^2\right]$$

I **average ionization potential**

W **maximum energy loss**

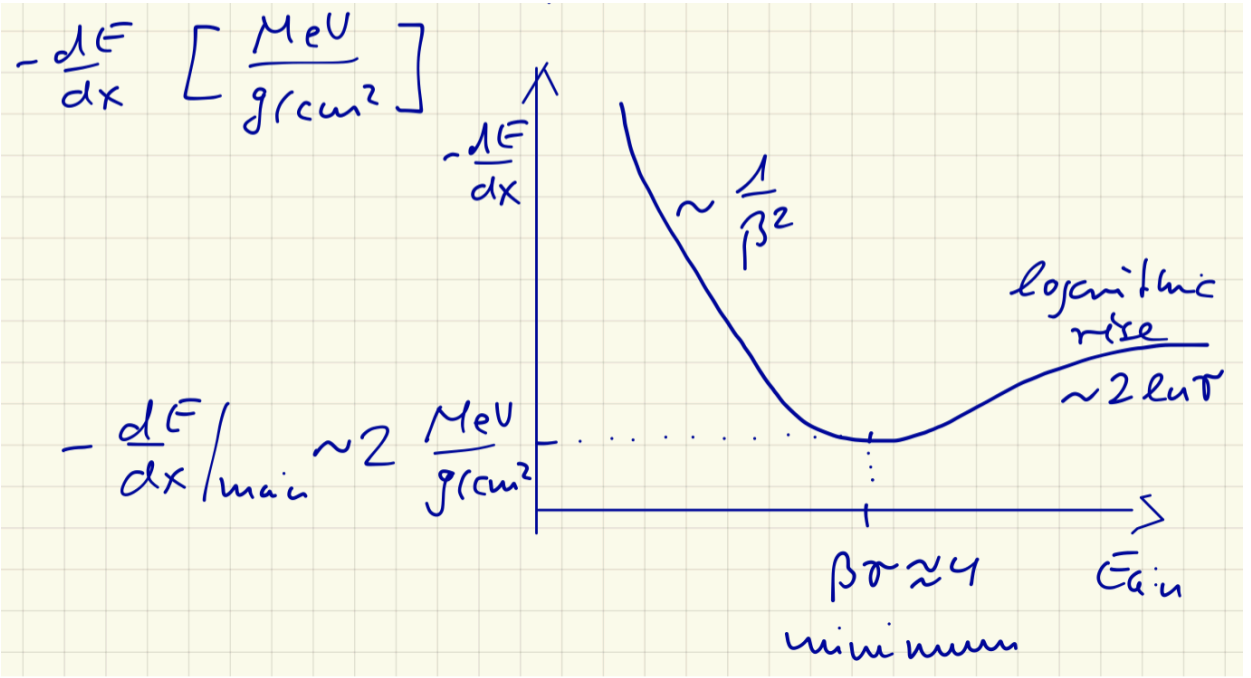

the ionization loss is proportional to a constant L that includes the charge and atomic number fo the medium

$$L = \frac{2\pi N_A Z}{A}\left(\frac{e^2}{mc^2}\right)^2 mc^2 = 0.0765\left(\frac{2Z}{A}\right)$$ **MeV/(g cm²)**

for dense media: reduction of logarithmic rise (density effect)

$$\frac{dE}{dx} = -L\frac{Z^2}{\beta^2}\left(B + 0.69 + 2\ln\gamma\beta + \ln W - 2\beta^2 - \delta\right)$$ **MeV/(g cm²)**

$$B = \ln\left(\frac{mc^2}{I}\right) \qquad W \approx \frac{E}{2}$$

$$\delta = 2\ln\gamma\beta + C$$

***C* correction factor (Sternheimer)**

element	I, eV	L	B	C
hydrogen	21.8	152	21.07	-9.50
helium	44.0	77	19.39	-2.13
carbon	77.8	77	18.25	-3.22
nitrogen	90.0	77	17.67	-10.68
oxygen	104	77	17.67	-10.80
iron	286	72	15.32	-4.62

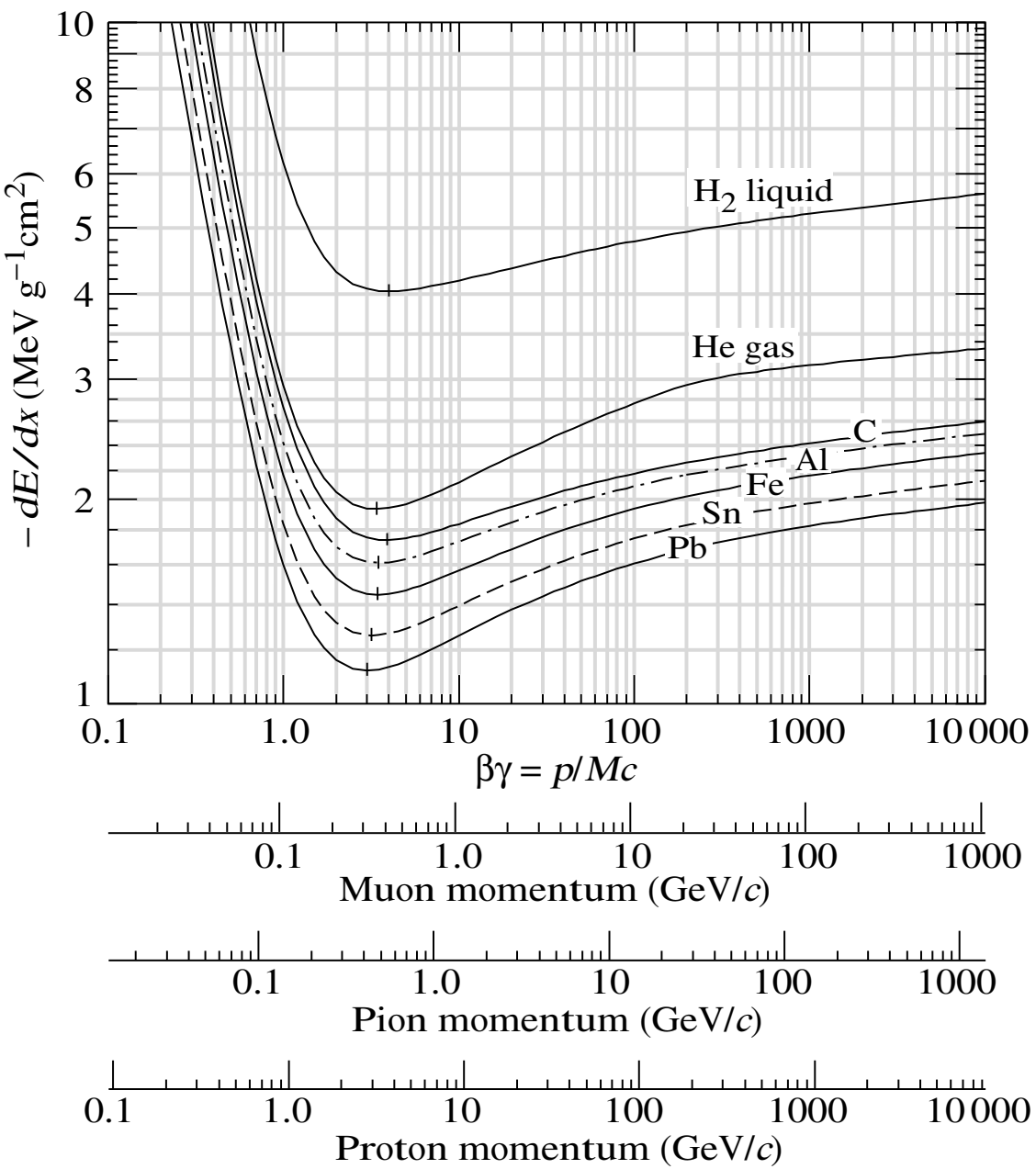

Figure 27.2: Mean energy loss rate in liquid (bubble chamber) hydrogen, gaseous helium, carbon, aluminum, iron, tin, and lead. Radiative effects, relevant for muons and pions, are not included. These become significant for muons in iron for $\beta\gamma \gtrsim 1000$, and at lower momenta for muons in higher-Z absorbers. See Fig. 27.21.

Bethe Bloch gives mean energy loss
thin absorbers: large fluctuations
energy loss can be described by a Landau function

$$\mathcal{L}(x) = \frac{1}{\sqrt{2\Gamma}} \exp\left(-\frac{1}{2}(\lambda + e^{-\lambda})\right)$$

$$\lambda = \frac{\Delta E - \Delta E^{mp}}{\xi}$$

$$\xi = \kappa \cdot \rho \cdot x$$

ΔE **true energy loss in layer**

ΔE^{mp} **most probable energy loss in layer**

x **thickness of absorber [cm]**

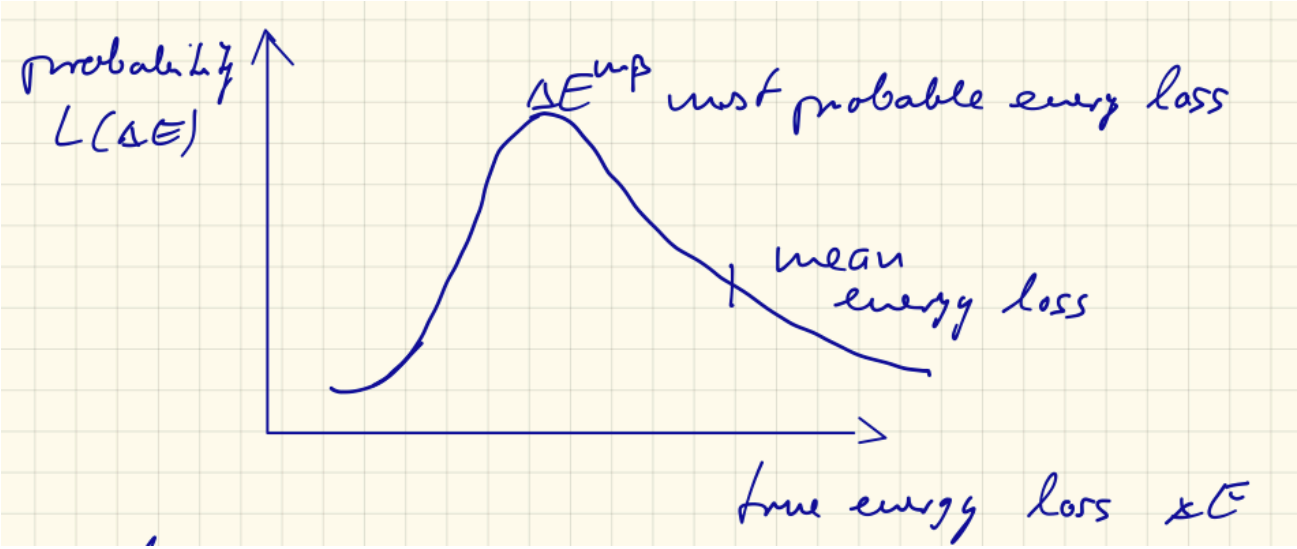

for electrons in Argon

$$\Delta E^{mp} = \xi \left\{ \ln \left[\frac{2 m_e c^2 \gamma^2 \beta^2}{I^2} \xi \right] - \beta^2 + 0.423 \right\}$$

energy loss of MIP $\beta\gamma \approx 4$

1 cm argon ΔE^{mp} **= 1.2 keV** $\Delta E_{BB} = 2.69$ **keV**

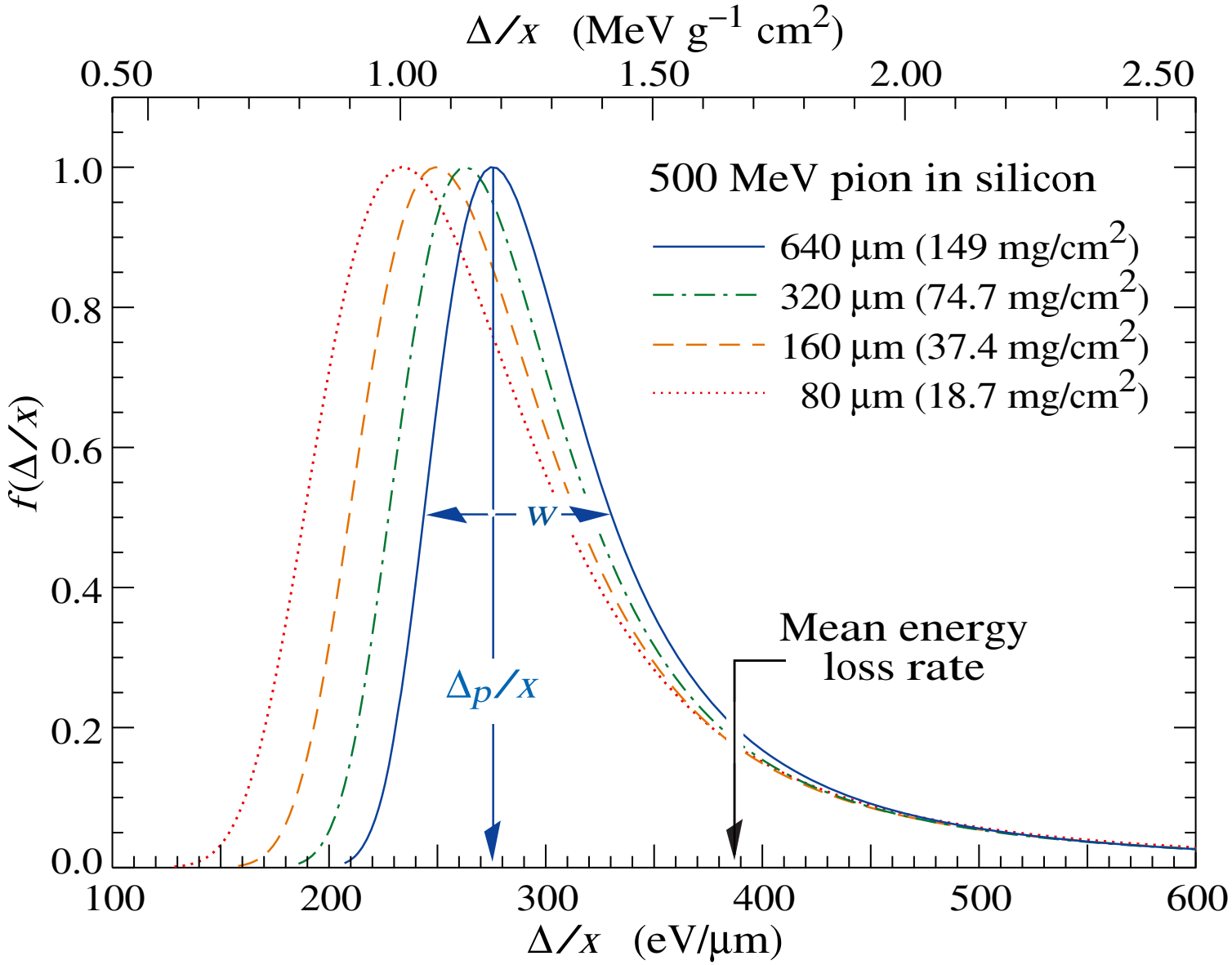

Figure 27.7: Straggling functions in silicon for 500 MeV pions, normalized to unity at the most probable value δ_p/x. The width w is the full width at half maximum.

Cherenkov radiation

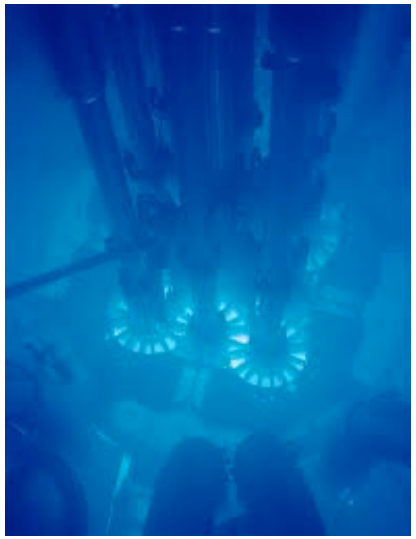

charged particles, moving in a medium with refractive index n with

$$v > \frac{c}{n}$$

emit electromagnetic radiation --> Cherenkov radiation

electrons passing through a dielectric at

$v < \frac{c}{n}$

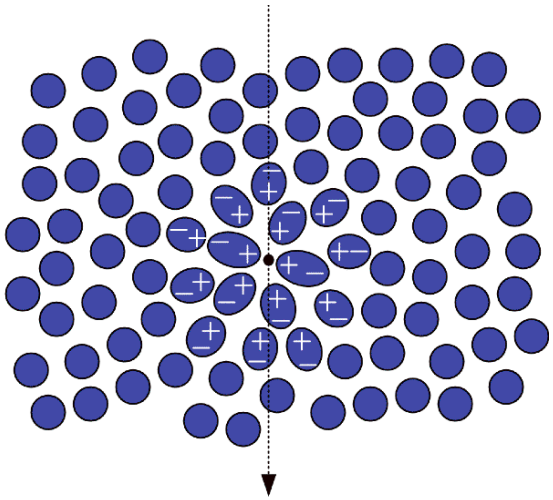

$v > \frac{c}{n}$

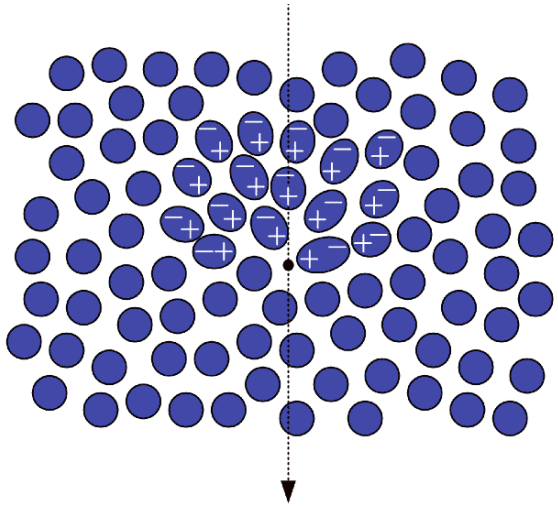

Charged particles, passing by the atoms in the dielectric, momentarily polarize them. Once the particle has passed, this polarized state collapses, causing each atom to emit Cerenkov radiation. For slow moving particles, the polarization is perfectly symmetrical, resulting in no electric field at long distances. When the particle is moving very quickly, however, the polarization is no longer perfectly symmetrical.

Cherenkov radiation

angle between the trajectory of the particle and the emitted photons

$$\cos\theta_c = \frac{c}{n\beta c} = \frac{1}{n\beta}$$

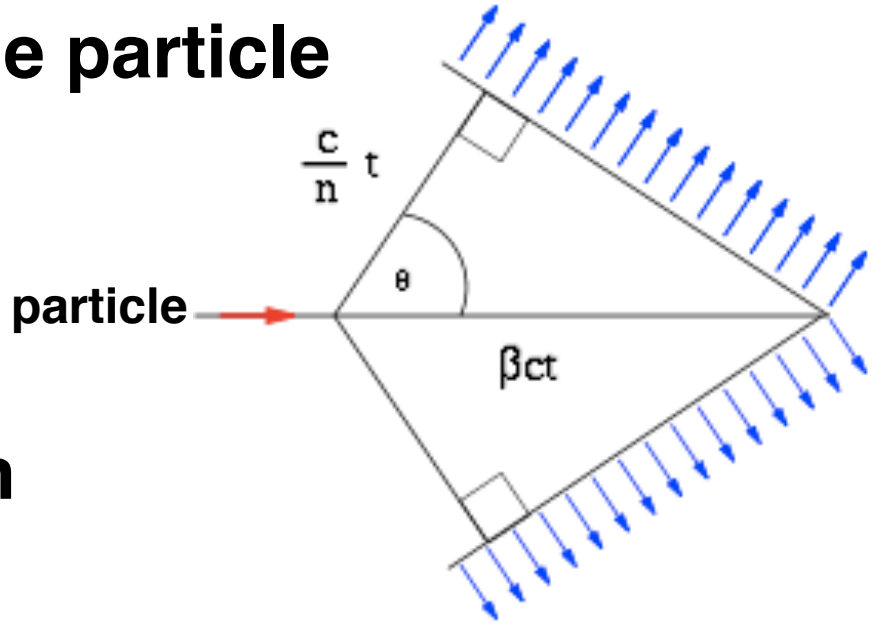

threshold for Cherenkov radiation

$$\beta > \frac{1}{n}$$

at threshold, the photons are emitted in forward direction

the Cherenkov angle increases to a maximum value for $\beta = 1$**:** $\theta_c = \arccos\frac{1}{n}$

threshold energy

$$\gamma_{th} = \frac{1}{\sqrt{1-\beta_{th}^2}} = \frac{1}{\sqrt{1-\frac{1}{n^2}}} \quad \text{with} \quad \gamma_{th} = \frac{E_{th}}{m_o c^2}$$

Cherenkov radiation

intensity of Cherenkov radiation per unit path length

$$\frac{dN}{dL} = z^2 \frac{\alpha}{\hbar c}\left[1 - \frac{1}{\beta^2 n^2}\right] \qquad \frac{\alpha}{\hbar c} = 370/\text{(eV cm)}$$

Bremsstrahlung

charged particles also interact with the electromagnetic field of the atomic nuclei and generate photons

the energy loss on bremsstrahlung is

$$\frac{dE}{dx} = -\frac{N}{A}\int_0^{E-mc^2} \sigma_{br}(E,k)k\,dk$$

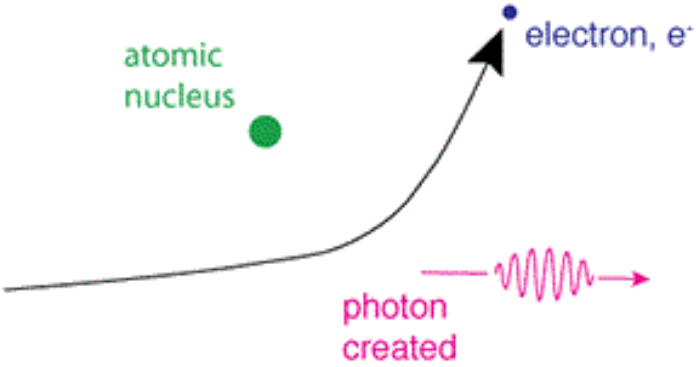

E **energy of charged particle** ***k*** **energy of photon**

cross section $\sigma_{br} = \frac{4Z^2\alpha r_e^2}{k}F(E,k)$

$r_e = \frac{e^2}{\hbar c}$ **classical electron radius**

F(E,k) **depends on the screening parameter, which expresses the screening of the nuclear field by the atomic electrons**

$$\xi = 100Mc^2\frac{k}{E}\frac{1}{E-k}Z^{-1/3}$$

Bremsstrahlung

the screening parameter is inversely proportional to the energy of the charged particle and is proportional to the ratio of the electron energy before and after the process

ratio of the photon to electron energy *u=k/E*

$$F(E,k) = \left[4\frac{1-u}{3} + u^2\right] \ln Z^{-1/3} + \frac{1-u}{9}$$

for high-energy electrons with $\xi \approx 0$

the energy loss is then

$$\frac{dE}{dx} = \frac{4NZ}{A}\alpha r_e^2 E \left[\ln 191 Z^{-1/3} + \frac{1}{18}\right]$$

the correction factor 1/18 is due to the interactions with the fields of the atomic electrons

radiation length

the general form of the energy loss allows the introduction of the radiation length X_0

$$X_0 = \left[\frac{4NZ(Z+1)}{A} \alpha r_e^2 E \ln(191 Z^{-1/3}) \right]^{-1}$$

it gives the average amount of matter for bremsstrahlung energy loss

approximate values can be calculated by

$$X_0 \approx 10^3 \frac{A}{6Z(Z+1)} \quad \text{g/cm}^2$$

for mixtures: weighted sum

$$\frac{1}{X_0} = \sum_i \frac{w_i}{X_0^i}$$

Table 2.4. Radiation lengths and critical energies for the most common elements. The radiation length values are from [11] and the critical energies from [3].

Element	Z	A	X_0, g/cm^2	ε_0, MeV
Hydrogen	1	1.01	61.28	350.
Helium	2	4.00	94.52	250.
Carbon	6	12.01	42.70	79.
Nitrogen	7	14.01	37.99	85.
Oxygen	8	16.00	34.24	75.
Silicon	14	28.09	28.08	37.5
Iron	26	55.85	13.84	20.7

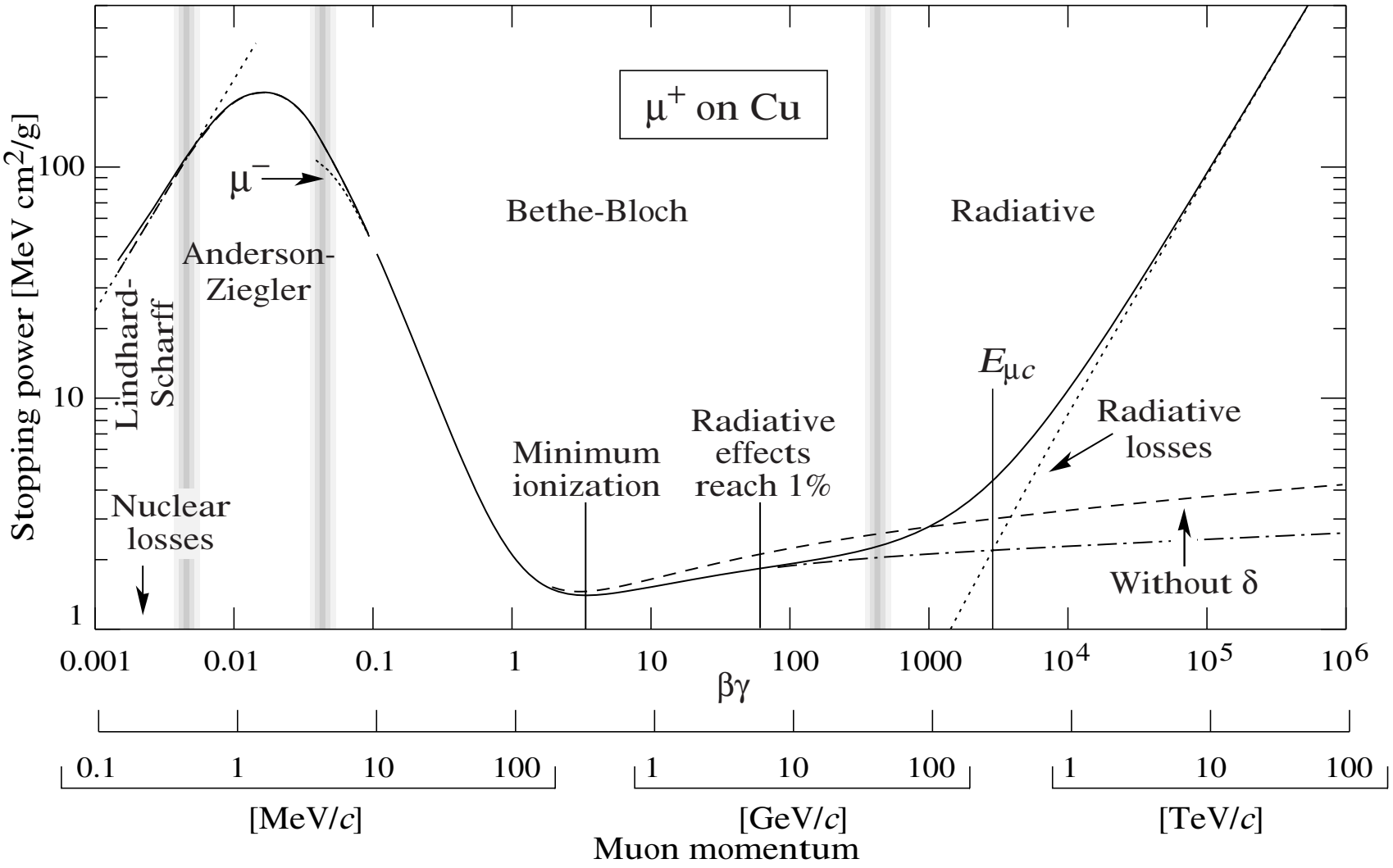

Fig. 27.1: Stopping power ($= \langle -dE/dx \rangle$) for positive muons in copper as a function of $\beta\gamma = p/Mc$ over nine orders of magnitude in momentum (12 orders of magnitude in kinetic energy). Solid curves indicate the total stopping power. Data below the break at $\beta\gamma \approx 0.1$ are taken from ICRU 49 [4], and data at higher energies are from Ref. 5. Vertical bands indicate boundaries between different approximations discussed in the text. The short dotted lines labeled "μ^-" illustrate the "Barkas effect," the dependence of stopping power on projectile charge at very low energies [6].

critical energy

critical energy E_c

$$-\left.\frac{dE}{dx}(E_c)\right|_{\text{ionization}} = -\left.\frac{dE}{dx}(E_c)\right|_{\text{brems}}$$

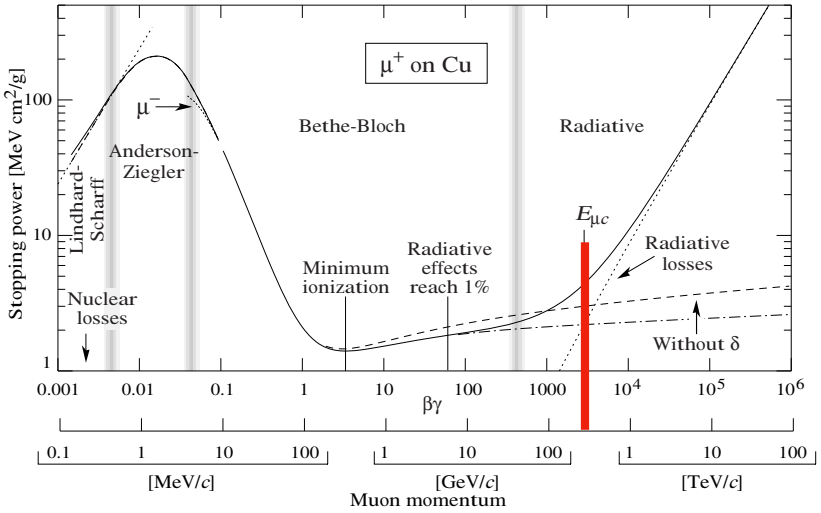

empirical parameterizations

$$E_c \approx \frac{610\ \text{MeV}}{Z + 1.24} \quad \textbf{(solids)}$$

$$E_c \approx \frac{710\ \text{MeV}}{Z + 0.92} \quad \textbf{(gases)}$$

E_c scales with mass of projectile

$$E_c^{\mu} \approx E_c^{e} \left(\frac{m_{\mu}}{m_e}\right)^2$$

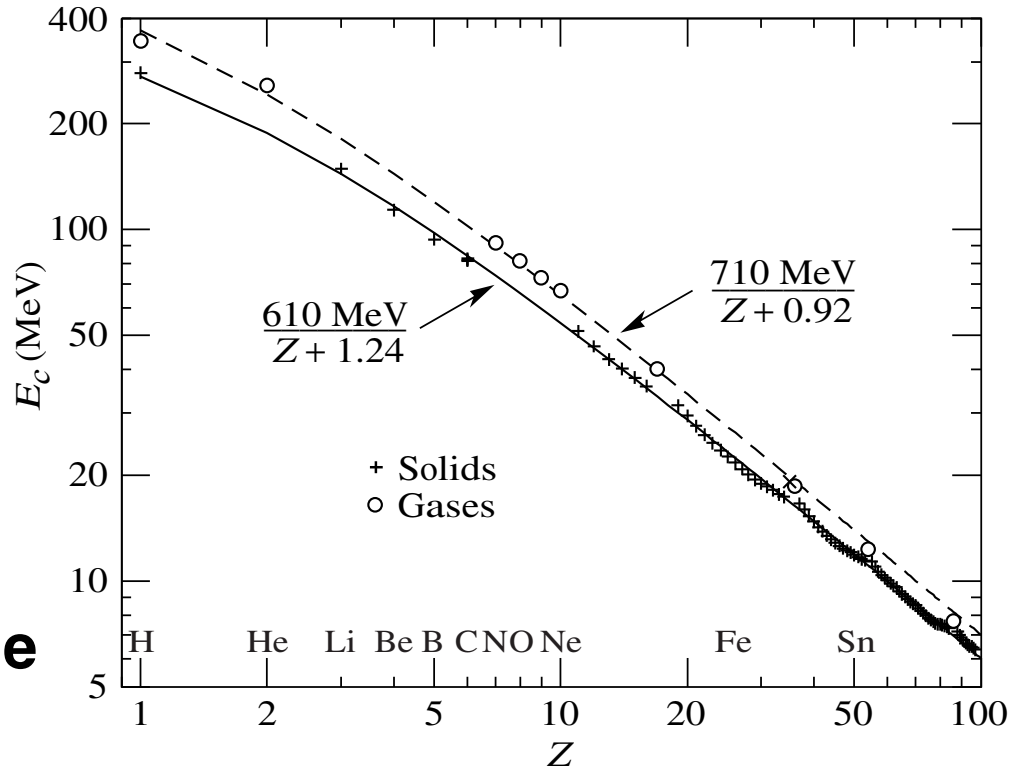

Figure 27.13: Electron critical energy for the chemical elements, using Rossi's definition [2]. The fits shown are for solids and liquids (solid line) and gases (dashed line). The rms deviation is 2.2% for the solids and 4.0% for the gases. (Computed with code supplied by A. Fassó.)

Interaction of photons

To register photons we need to produce charged particles.
This is significantly different from ionization for charged particles.

Photons are absorbed: photo effect, undergo pair production, or scattered with large angles: Compton effect

attenuation of photons in matter $I = I_0 \exp(-\mu x)$

absorption coefficient $\mu = \frac{N_A}{A} \sum_i \sigma_i \left[\frac{g}{cm^2}\right]$

σ_i **cross section for species *i***

Photo(electric) effect

electrons in atoms can fully absorb E_γ

(not possible for free e **due to momentum conservation)**

total photo-electric cross section

$$\sigma^K_{photo} = \sqrt{\frac{32}{\epsilon^7}}\alpha^4 Z^5 \sigma^e_{Th} \qquad \left[\frac{cm^2}{Atom}\right]$$

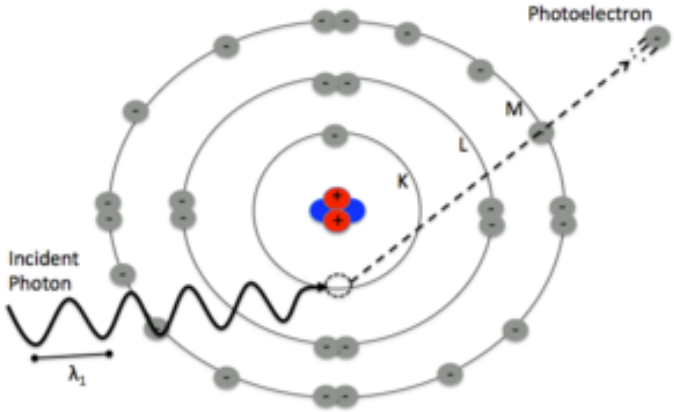

$$\epsilon = \frac{E_\gamma}{m_e c^2}$$ **reduced photon energy**

q **in the notation of Stanev**

Thomson cross section for elastic scattering of photons at electrons

$$\sigma^e_{Th} = \frac{8}{3}\pi r_e^2 = 6.65 \cdot 10^{-25}\mathrm{cm}^2$$

for $\epsilon >> 1$

$$\sigma^K_{Ph} = 4\pi r_e^2 Z^5 \alpha^4 \frac{1}{\epsilon}$$

$$\sigma^K_{Ph} \propto Z^5$$ **--> interaction with more than one electron in the atom**

Compton effect

photons interact with atomic electrons and transfer a fraction of their energy to the electrons

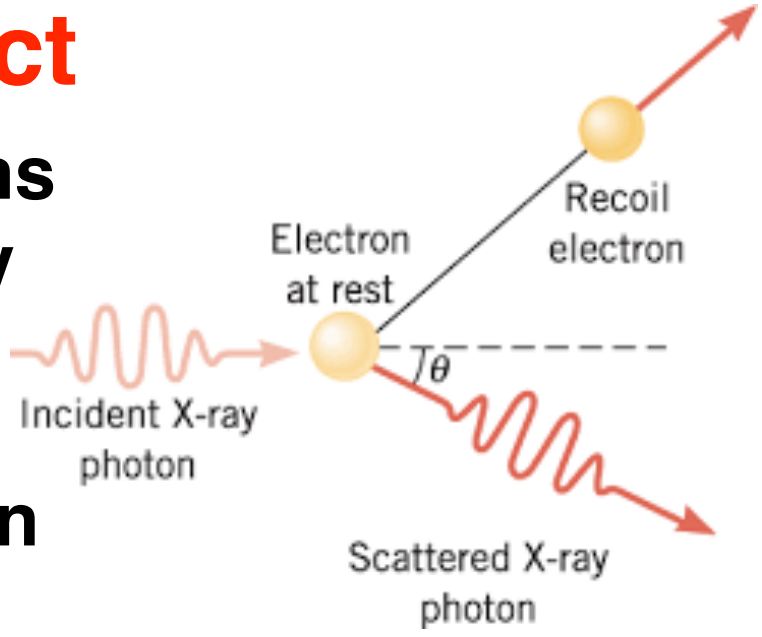

differential cross section for Compton scattering of a photon of energy *k*

$$\sigma_C(k,k') = 2\pi r_e^2 \frac{1}{k'}\frac{1}{q}\left[1 + \left(\frac{k'}{k}\right)^2 - \frac{2(q+1)}{q^2} + \frac{1+2q}{q^2}\frac{k'}{k} + \frac{1}{q^2}\frac{k}{k'}\right]$$

***k'* photon energy after scattering**
***q* is photon energy in units of electron mass $q=k/m\,c^2$**

integrating over all *k'* gives

$$\sigma_C(k) = \frac{\pi r_e^2}{q}\left[\left(1 - \frac{2(q+1)}{q^2}\right)\ln(2q+1) + \frac{1}{2} + \frac{4}{q} - \frac{1}{2(2q+1)^2}\right]$$

Compton effect

at low q values σ_C approaches the Thomson cross section $\sigma_T = 8\pi r_e^2/3 = 665\text{mb}$

and decreases with increasing energy

for k much greater than the electron mass, the cross section is well represented by the much simpler formula

$$\sigma_C \approx \sigma_T \frac{3}{8q}\left(\ln 2q + \frac{1}{2}\right)$$

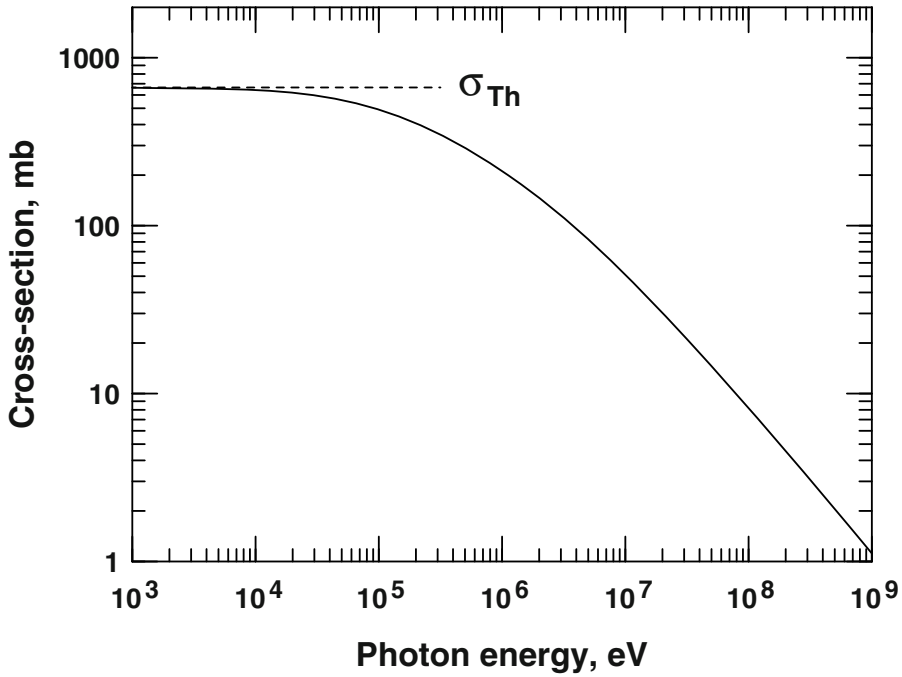

Fig. 2.1. Cross-section for Compton scattering as a function of the photon energy.

Compton effect

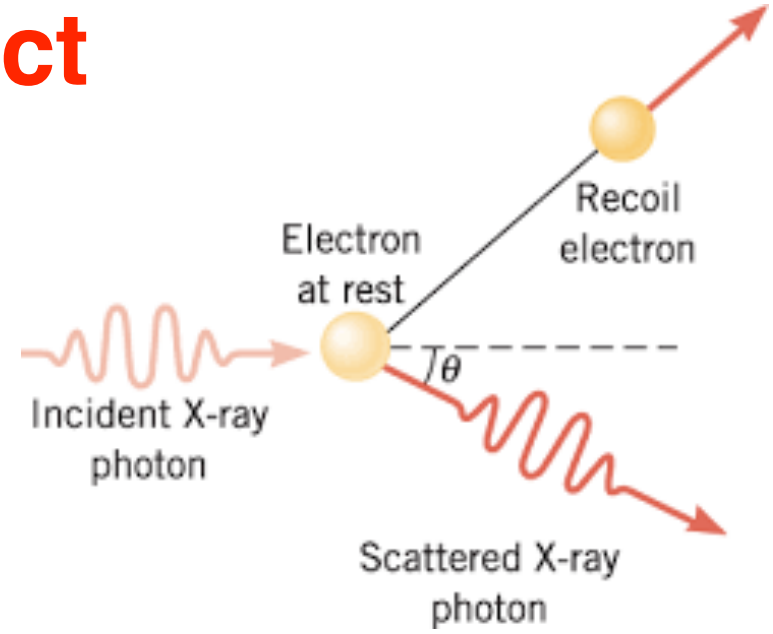

the angle between the primary and the secondary photon can be expressed as a function of the energies of the photon before and after the scattering

$$\cos\Theta = 1 - \frac{mc^2(k/k' - 1)}{k}$$

Pair production

The inverse process of bremsstrahlung

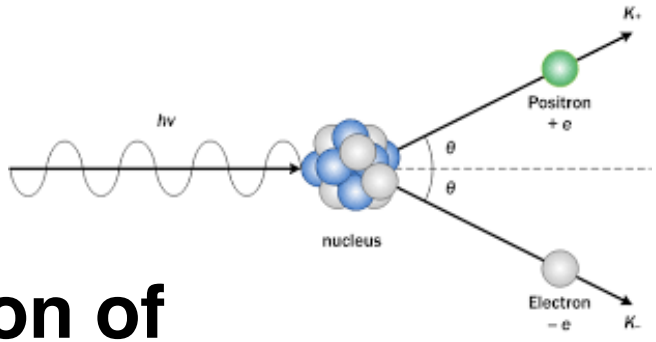

The cross section can be calculated by substituting the electron and the positron of the pair for the electron before and after bremsstrahlung

$$\sigma_{pair}(k,E) = \sigma_{br}(E,k)\frac{E^2}{k^2} = \frac{4Z^2\alpha r_e^2}{k}G(k,E)$$

k **is the energy of the primary photon**

the function ***G(k,E)*** **can be expressed as a function of the ratio** ***v=E/k***

E **is the energy of one of the members of the pair**

Pair production

the shape of *G(k,E)* also depends on the screening parameter

for the case of full screening

$$G(k,v) = [1 + 4v(v-1)/3] \ln(191 Z^{-1/3}) - v(1-v)/9$$

for the case of no screening

$$G(k,v) = [1 + 4v(v-1)/3] \left[\ln\left(\frac{2k}{mc^2}\right) v(1-v) - \frac{1}{2} \right]$$

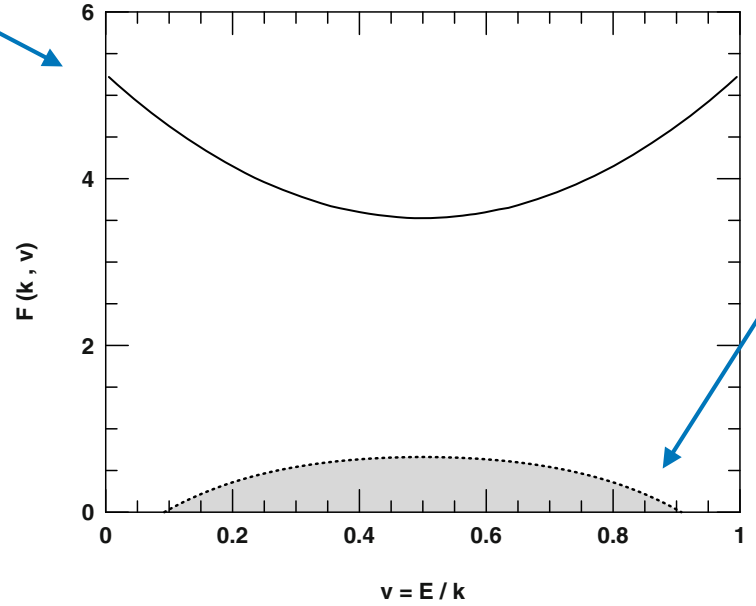

Fig. 2.3. $G(E,k)$ from (2.23) (solid line) and (2.24) (dotted line, shaded areas) for primary photon energy 100 MeV.

Pair production

the total pair production cross section can be directly integrated

$$\sigma_{pair}(k) = \int_{mc^2}^{k-mc^2} \sigma_{pp}(k,E)\,dE$$

$$= 4Z^2\alpha r_e^2 \frac{\ln\left(191Z^{-1/3}\right)}{9} - \frac{1}{54} \quad \left[\frac{\mathrm{cm}^2}{\mathrm{atom}}\right]$$

in the case of vanishing ξ

the correction 1/54 comes from pair production in the field of the atomic electrons

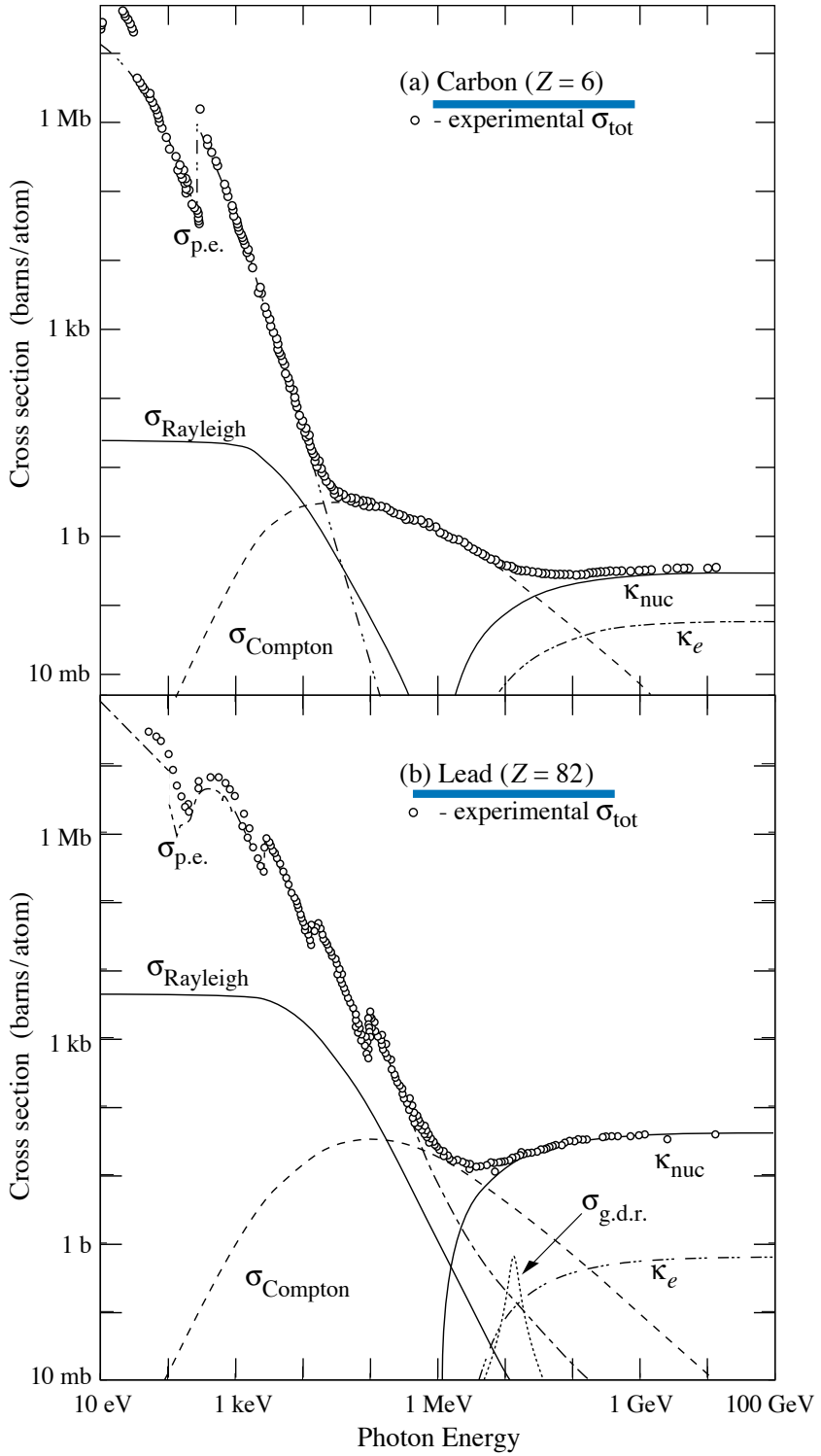

Figure 27.14: Photon total cross sections as a function of energy in carbon and lead, showing the contributions of different processes:

$\sigma_{\text{p.e.}}$ = Atomic photoelectric effect (electron ejection, photon absorption)

σ_{Rayleigh} = Rayleigh (coherent) scattering–atom neither ionized nor excited

σ_{Compton} = Incoherent scattering (Compton scattering off an electron)

κ_{nuc} = Pair production, nuclear field

κ_e = Pair production, electron field

$\sigma_{\text{g.d.r.}}$ = Photonuclear interactions, most notably the Giant Dipole Resonance [48]. In these interactions, the target nucleus is broken up.

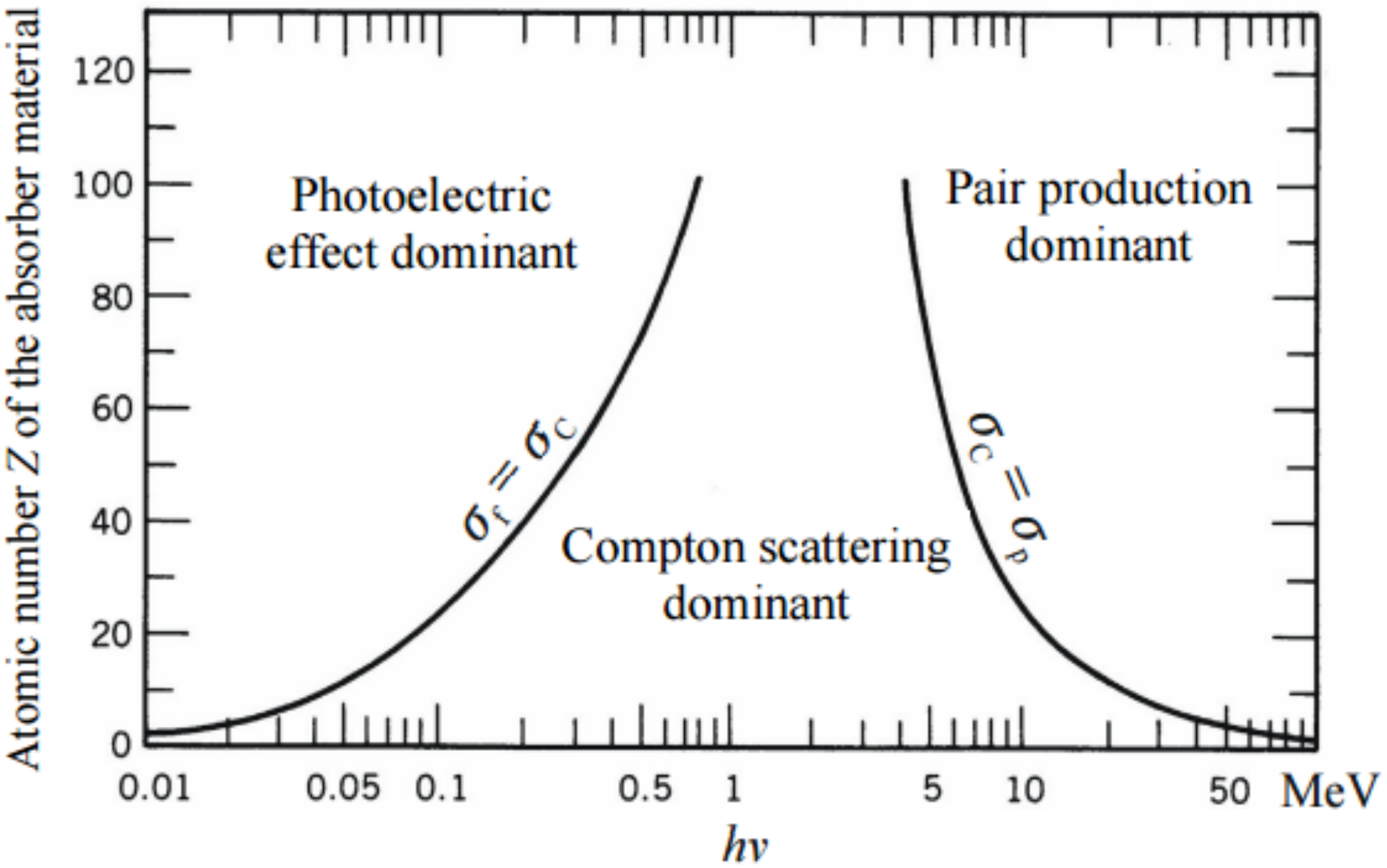
Atomic number Z of the absorber material
120
100
80
60
40
20
0
Photoelectric
effect dominant
Pair production
dominant
Compton scattering
dominant
$\sigma_\tau = \sigma_C$
$\sigma_C = \sigma_p$
0.01
0.05
0.1
0.5
1
5
10
50
MeV
$h\nu$

Synchrotron radiation

important energy loss process for charged particles in presence of magnetic fields

An electron moving in the magnetic field B with an angle θ to the field direction loses energy to synchrotron radiation at a rate

$$-\frac{dE}{dt} = 2\sigma_T c\gamma^2 U_B \beta^2 \sin^2\theta \ ,$$

$U_B = \dfrac{B^2}{8\pi}$ **energy density of magnetic field**

σ_T **Thomson cross section**

synchrotron energy loss is proportional to γ^2

and thus proportional to $\dfrac{1}{m^2}$

for particles with the same E_{tot}

Synchrotron radiation

for an ensemble of electrons that are scattered randomly in all directions, the energy loss averaged over all pitch angles is

$$\left\langle -\frac{dE}{dt} \right\rangle = \frac{4}{3}\sigma_T c \gamma^2 U_B$$

for relativistic electrons $\beta \simeq 1$

average energy loss (in particle physics units)

$$-\frac{dE}{dt} = 3.79 \times 10^{-6} \left(\frac{B}{\text{gauss}}\right)^2 \left(\frac{E_e}{\text{GeV}}\right)^2 \text{GeV/s}$$

the characteristic frequency of the radiated photons is the critical frequency

$$\nu_c = \frac{3}{4\pi}\gamma^2 \frac{eB}{m_e c} \sin\theta = 1.61 \times 10^{13} \left(\frac{B}{\text{gauss}}\right) \left(\frac{E}{\text{GeV}}\right)^2 \text{Hz}\,.$$

Synchrotron radiation

the emissivity of a relativistic electron of energy E_e averaged over all pitch angles is given by the integral

$$j(E,\nu)\,d\nu = \frac{\sqrt{3}e^3 B}{m_e c^2}\int_0^{\pi} d\theta\,\sin^2\theta/2(\nu/\nu_c)\,d\nu\int_{\nu/\nu_c}^{\infty} K_{5/3}(\eta)\,d\eta\ ,$$

$K_{5/3}$ is the Bessel function of order 5/3.

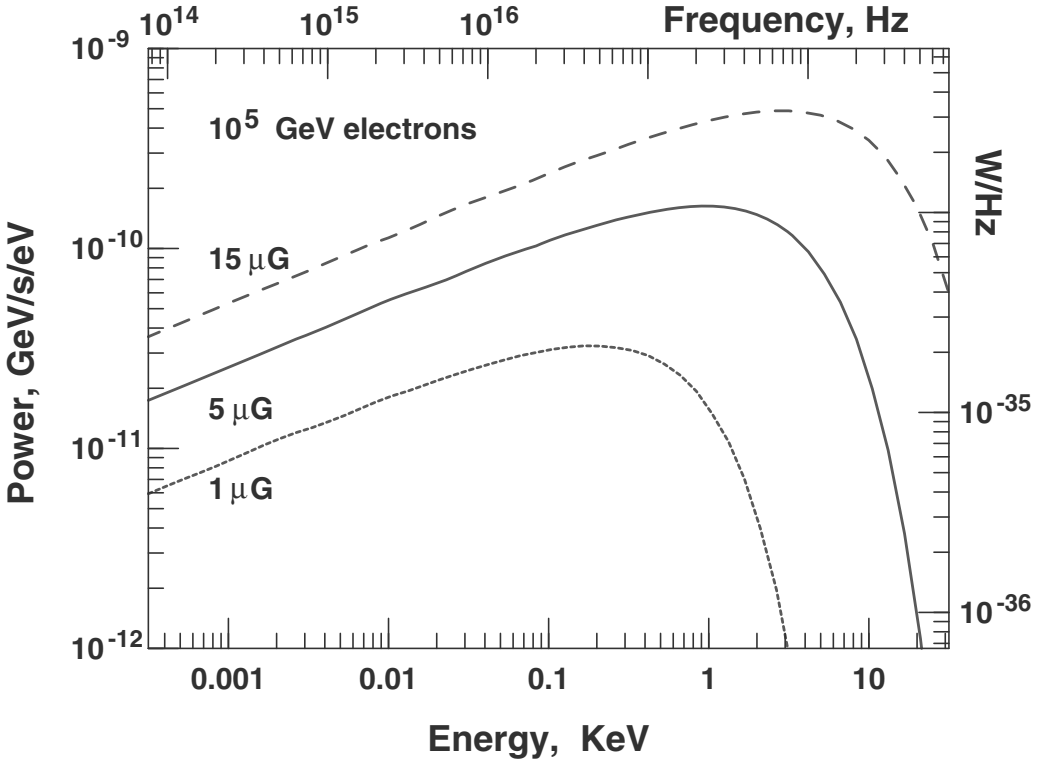

the number spectrum of the synchrotron radiation peaks at $0.29\nu_c$

Fig. 2.4. Power spectrum of synchrotron radiation emitted by 10^5 GeV electrons in 1, 5, and 15 μG fields.

Inverse Compton effect

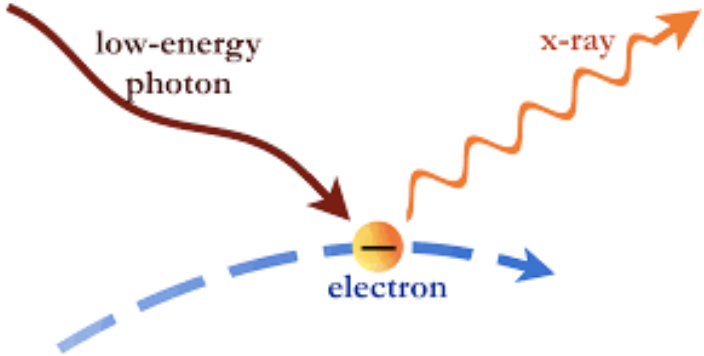

important in astrophysics

e transfers energy to γ

we can use the equations from the Compton effect (see above)

energy of primary electron E

assumed to be $m_e c^2$ in the equation above

and the energy of the ambient photon ϵ are used to represent the photon energy in the electron rest frame

$$k = \frac{\epsilon E}{m_e c^2}(1 - \beta \cos\theta) \,,$$

Inverse Compton effect

very important process for the production of very high-energy gamma rays, when accelerated electrons collide with ambient photons

In the Thomson regime $\epsilon E \ll (m_e c^2)^2$

the average energy of the boosted photon is

$$E_\gamma = \epsilon (E/m_e c^2)^2$$

and the cross section is roughly σ_T

Inverse Compton effect

using these estimates we can write the energy loss formulae for the electrons

in the Thomson regime

$$-\frac{dE}{dx} = \sigma_T U \left(\frac{E}{m_e c^2}\right)^2$$

U is the energy density of the photon field

in the high-energy regime (Klein-Nishima)

$$-\frac{dE}{dx} = \frac{3}{8}\sigma_T U \left(\frac{m_e c^2}{\epsilon}\right)^2 \ln\left(\frac{2\epsilon E}{m_e^2 c^4}\right)$$

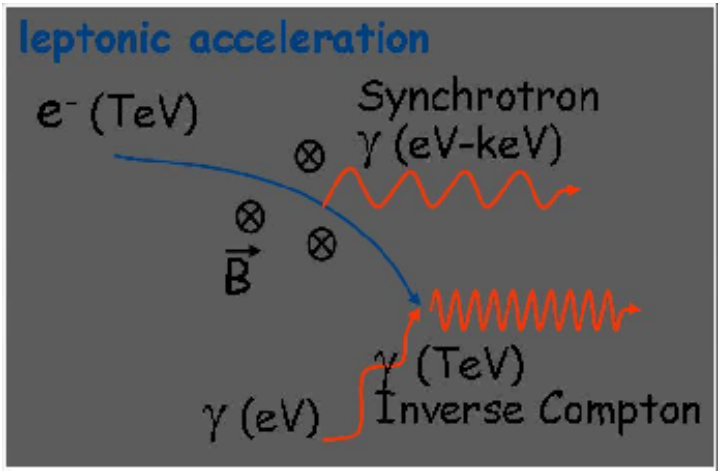

important for astrophysics: synchrotron self Compton

Inelastic hadronic interactions

A particle of mass m that moves at a velocity βc is characterized by a four vector p

$$p\,(p_x,\,p_y,\,p_z) - \mathrm{p}^2 \;=\; E^2 - |\boldsymbol{p}|^2 \;=\; m^2$$

its relative velocity $\beta \;=\; \boldsymbol{p}/E$

and its Lorentz factor $\gamma \;=\; (1 \,-\, \beta^2)^{-1/2} \;=\; E/m.$

it is convenient to discuss hadronic interactions in the center of mass system

$$\sqrt{s} \;=\; (\mathrm{p}_1 + \mathrm{p}_2)^2 \;=\; \left[(E_1 + E_2)^2 \,-\, (\boldsymbol{p}_1 - \boldsymbol{p}_2)^2\right]^{1/2}$$

or, when one of the particles is at rest

$$\sqrt{s} \;=\; (m_1^2 + m_2^2 + 2m_2 E_1^{Lab})^{1/2}$$

E_1^{lab} is energy of incident particle in rest frame of particle 2

Inelastic hadronic interactions

in an inelastic hadronic interaction at least one new (secondary) particle is produced

$\sqrt{s}$ has to be large enough to accommodate the mass of the secondary particle

e.g. if two protons collide and produce a neutral pion

$$p + p \longrightarrow p + p + \pi^0 \qquad \sqrt{s} > 2m_p + m_\pi = 2.01 \text{ GeV}.$$

minimum energy of proton in rest frame is

$$E_1 = s/2m_p - m_p = 1.22 \text{ GeV}.$$

Inelastic hadronic interactions

the cross section for inelastic interactions depends on the incident particle energy

PRL 109, 062002 (2012) PHYSICAL REVIEW LETTERS week ending 10 AUGUST 2012

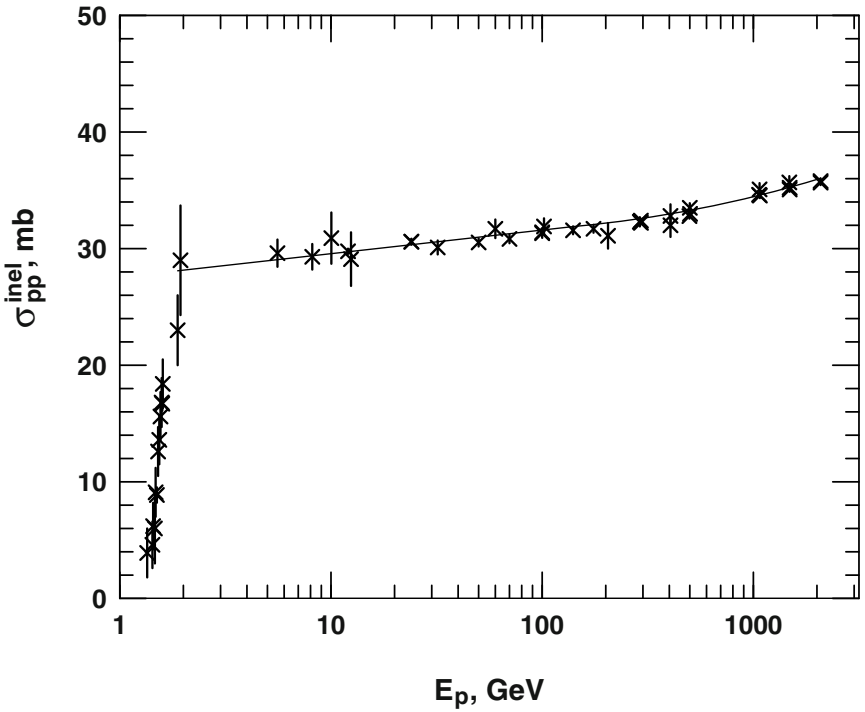

Fig. 2.5. Results from direct accelerator measurements of the *pp* inelastic cross-section. The data points are from the compilation of Ref. [17] and the line is the fit from Ref. [18].

Measurement of the Proton-Air Cross Section at $\sqrt{s} = 57$ TeV with the Pierre Auger Observatory

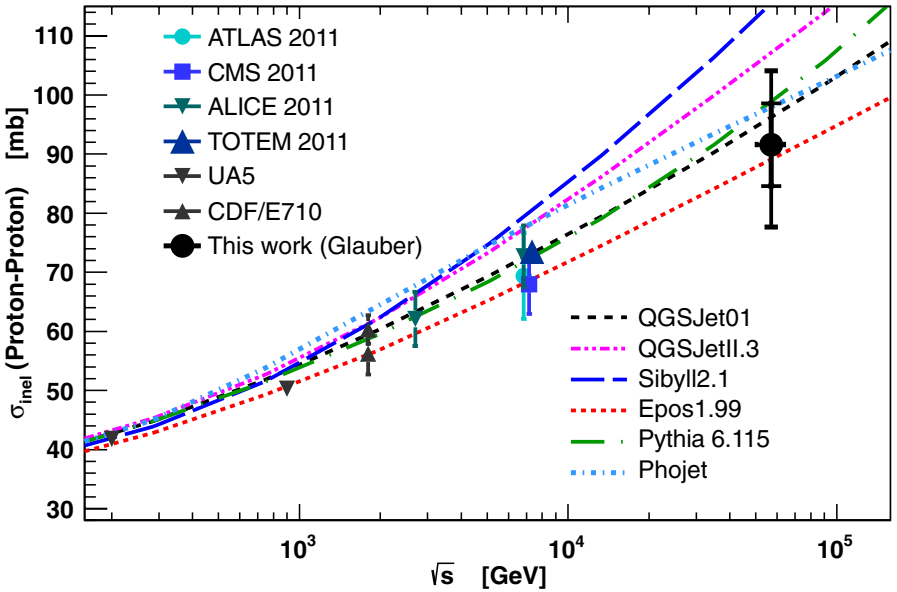

FIG. 4 (color online). Comparison of derived $\sigma_{pp}^{\text{inel}}$ to model predictions and accelerator data [29]. Here we also show the cross sections of two typical high-energy models, PYTHIA6 [35] and PHOJET [36]. The inner error bars are statistical, while the outer include systematic uncertainties.

Strong interaction of hadrons

in addition to electromagnetic interactions of charged particles in inelastic processes --> production of particles

$$\sigma_{tot} = \sigma_{elastic} + \sigma_{inelastic}$$

for inelastic processes: absorption length λ_a

absorption of hadrons in matter $N = N_0 \exp\left(-\frac{x}{\lambda_a}\right)$

$$\lambda_a = \frac{A}{N_A \cdot \rho \cdot \sigma_{inelastic}} \quad [\mathrm{cm}] \qquad A\left[\frac{\mathrm{g}}{\mathrm{mol}}\right] \quad N_a\left[\frac{1}{\mathrm{mol}}\right] \quad \rho\left[\frac{\mathrm{g}}{\mathrm{cm}^3}\right]$$

$$\lambda_a \cdot \rho \rightarrow \left[\frac{\mathrm{g}}{\mathrm{cm}^2}\right]$$

interaction length $\lambda_{int} = \frac{A}{N_A \cdot \rho \cdot \sigma_{tot}}$

$$\sigma_{tot} > \sigma_{inelastic} \rightarrow \lambda_{int} < \lambda_a$$

for material with $Z > 6 \quad \text{and} \quad \lambda_a > X_0$

6. ATOMIC AND NUCLEAR PROPERTIES OF MATERIALS

Table 6.1 Abridged from `pdg.lbl.gov/AtomicNuclearProperties` by D. E. Groom (2007). See web pages for more detail about entries in this table including chemical formulae, and for several hundred other entries. Quantities in parentheses are for NTP (20° C and 1 atm), and square brackets indicate quantities evaluated at STP. Boiling points are at 1 atm. Refractive indices n are evaluated at the sodium D line blend (589.2 nm); values $\gg 1$ in brackets are for $(n-1)\times 10^6$ (gases).

Material	Z	A	$\langle Z/A\rangle$	Nucl.coll. length λ_T {g cm^{-2}}	Nucl.inter. length λ_I {g cm^{-2}}	Rad.len. X_0 {g cm^{-2}}	$dE/dx\|_{\rm min}$ { MeV g^{-1}cm^2}	Density {g cm^{-3}} ({gℓ^{-1}})	Melting point (K)	Boiling point (K)	Refract. index (@ Na D)
H_2	1	1.00794(7)	0.99212	42.8	52.0	63.04	(4.103)	0.071(0.084)	13.81	20.28	1.11[132.]
D_2	1	2.01410177803(8)	0.49650	51.3	71.8	125.97	(2.053)	0.169(0.168)	18.7	23.65	1.11[138.]
He	2	4.002602(2)	0.49967	51.8	71.0	94.32	(1.937)	0.125(0.166)		4.220	1.02[35.0]
Li	3	6.941(2)	0.43221	52.2	71.3	82.78	1.639	0.534	453.6	1615.	
Be	4	9.012182(3)	0.44384	55.3	77.8	65.19	1.595	1.848	1560.	2744.	
C diamond	6	12.0107(8)	0.49955	59.2	85.8	42.70	1.725	3.520			2.42
C graphite	6	12.0107(8)	0.49955	59.2	85.8	42.70	1.742	2.210			
N_2	7	14.0067(2)	0.49976	61.1	89.7	37.99	(1.825)	0.807(1.165)	63.15	77.29	1.20[298.]
O_2	8	15.9994(3)	0.50002	61.3	90.2	34.24	(1.801)	1.141(1.332)	54.36	90.20	1.22[271.]
F_2	9	18.9984032(5)	0.47372	65.0	97.4	32.93	(1.676)	1.507(1.580)	53.53	85.03	[195.]
Ne	10	20.1797(6)	0.49555	65.7	99.0	28.93	(1.724)	1.204(0.839)	24.56	27.07	1.09[67.1]
Al	13	26.9815386(8)	0.48181	69.7	107.2	24.01	1.615	2.699	933.5	2792.	
Si	14	28.0855(3)	0.49848	70.2	108.4	21.82	1.664	2.329	1687.	3538.	3.95
Cl_2	17	35.453(2)	0.47951	73.8	115.7	19.28	(1.630)	1.574(2.980)	171.6	239.1	[773.]
Ar	18	39.948(1)	0.45059	75.7	119.7	19.55	(1.519)	1.396(1.662)	83.81	87.26	1.23[281.]
Ti	22	47.867(1)	0.45961	78.8	126.2	16.16	1.477	4.540	1941.	3560.	
Fe	26	55.845(2)	0.46557	81.7	132.1	13.84	1.451	7.874	1811.	3134.	
Cu	29	63.546(3)	0.45636	84.2	137.3	12.86	1.403	8.960	1358.	2835.	
Ge	32	72.64(1)	0.44053	86.9	143.0	12.25	1.370	5.323	1211.	3106.	
Sn	50	118.710(7)	0.42119	98.2	166.7	8.82	1.263	7.310	505.1	2875.	
Xe	54	131.293(6)	0.41129	100.8	172.1	8.48	(1.255)	2.953(5.483)	161.4	165.1	1.39[701.]
W	74	183.84(1)	0.40252	110.4	191.9	6.76	1.145	19.300	3695.	5828.	
Pt	78	195.084(9)	0.39983	112.2	195.7	6.54	1.128	21.450	2042.	4098.	
Au	79	196.966569(4)	0.40108	112.5	196.3	6.46	1.134	19.320	1337.	3129.	
Pb	82	207.2(1)	0.39575	114.1	199.6	6.37	1.122	11.350	600.6	2022.	
U	92	[238.02891(3)]	0.38651	118.6	209.0	6.00	1.081	18.950	1408.	4404.	
Air (dry, 1 atm)			0.49919	61.3	90.1	36.62	(1.815)	(1.205)		78.80	
Shielding concrete			0.50274	65.1	97.5	26.57	1.711	2.300			
Borosilicate glass (Pyrex)			0.49707	64.6	96.5	28.17	1.696	2.230			
Lead glass			0.42101	95.9	158.0	7.87	1.255	6.220			
Standard rock			0.50000	66.8	101.3	26.54	1.688	2.650			

6. ATOMIC AND NUCLEAR PROPERTIES OF MATERIALS

Table 6.1 Abridged from `pdg.lbl.gov/AtomicNuclearProperties` by D. E. Groom (2007). See web pages for more detail about entries in this table including chemical formulae, and for several hundred other entries. Quantities in parentheses are for NTP (20° C and 1 atm), and square brackets indicate quantities evaluated at STP. Boiling points are at 1 atm. Refractive indices n are evaluated at the sodium D line blend (589.2 nm); values $\gg 1$ in brackets are for $(n-1)\times 10^6$ (gases).

Material	Z	A	$\langle Z/A\rangle$	Nucl.coll. length λ_T {g cm^{-2}}	Nucl.inter. length λ_I {g cm^{-2}}	Rad.len. X_0 {g cm^{-2}}	$dE/dx\|_{\rm min}$ { MeV g^{-1}cm^2}	Density {g cm^{-3}} ({gℓ^{-1}})	Melting point (K)	Boiling point (K)	Refract. index (@ Na D)
Methane (CH_4)			0.62334	54.0	73.8	46.47	(2.417)	(0.667)	90.68	111.7	[444.]
Ethane (C_2H_6)			0.59861	55.0	75.9	45.66	(2.304)	(1.263)	90.36	184.5	
Propane (C_3H_8)			0.58962	55.3	76.7	45.37	(2.262)	0.493(1.868)	85.52	231.0	
Butane (C_4H_{10})			0.59497	55.5	77.1	45.23	(2.278)	(2.489)	134.9	272.6	
Octane (C_8H_{18})			0.57778	55.8	77.8	45.00	2.123	0.703	214.4	398.8	
Paraffin ($CH_3(CH_2)_{n\approx 23}CH_3$)			0.57275	56.0	78.3	44.85	2.088	0.930			
Nylon (type 6, 6/6)			0.54790	57.5	81.6	41.92	1.973	1.18			
Polycarbonate (Lexan)			0.52697	58.3	83.6	41.50	1.886	1.20			
Polyethylene ($[CH_2CH_2]_n$)			0.57034	56.1	78.5	44.77	2.079	0.89			
Polyethylene terephthalate (Mylar)			0.52037	58.9	84.9	39.95	1.848	1.40			
Polyimide film (Kapton)			0.51264	59.2	85.5	40.58	1.820	1.42			
Polymethylmethacrylate (acrylic)			0.53937	58.1	82.8	40.55	1.929	1.19			1.49
Polypropylene			0.55998	56.1	78.5	44.77	2.041	0.90			
Polystyrene ($[C_6H_5CHCH_2]_n$)			0.53768	57.5	81.7	43.79	1.936	1.06			1.59
Polytetrafluoroethylene (Teflon)			0.47992	63.5	94.4	34.84	1.671	2.20			
Polyvinyltoluene			0.54141	57.3	81.3	43.90	1.956	1.03			1.58
Aluminum oxide (sapphire)			0.49038	65.5	98.4	27.94	1.647	3.970	2327.	3273.	1.77
Barium flouride (BaF_2)			0.42207	90.8	149.0	9.91	1.303	4.893	1641.	2533.	1.47
Bismuth germanate (BGO)			0.42065	96.2	159.1	7.97	1.251	7.130	1317.		2.15
Carbon dioxide gas (CO_2)			0.49989	60.7	88.9	36.20	1.819	(1.842)			[449.]
Solid carbon dioxide (dry ice)			0.49989	60.7	88.9	36.20	1.787	1.563	Sublimes at 194.7 K		
Cesium iodide (CsI)			0.41569	100.6	171.5	8.39	1.243	4.510	894.2	1553.	1.79
Lithium fluoride (LiF)			0.46262	61.0	88.7	39.26	1.614	2.635	1121.	1946.	1.39
Lithium hydride (LiH)			0.50321	50.8	68.1	79.62	1.897	0.820	965.		
Lead tungstate ($PbWO_4$)			0.41315	100.6	168.3	7.39	1.229	8.300	1403.		2.20
Silicon dioxide (SiO_2, fused quartz)			0.49930	65.2	97.8	27.05	1.699	2.200	1986.	3223.	1.46
Sodium chloride (NaCl)			0.55509	71.2	110.1	21.91	1.847	2.170	1075.	1738.	1.54
Sodium iodide (NaI)			0.42697	93.1	154.6	9.49	1.305	3.667	933.2	1577.	1.77
Water (H_2O)			0.55509	58.5	83.3	36.08	1.992	1.000(0.756)	273.1	373.1	1.33
Silica aerogel			0.50093	65.0	97.3	27.25	1.740	0.200	(0.03 H_2O, 0.97 SiO_2)		

Nuclear fragmentation

nuclei are complex systems of protons and neutrons

in the liquid drop model the binding energy is defined as

$$\frac{E_b}{c^2} = \Delta M_A = Z m_p + N m_n - M_A$$

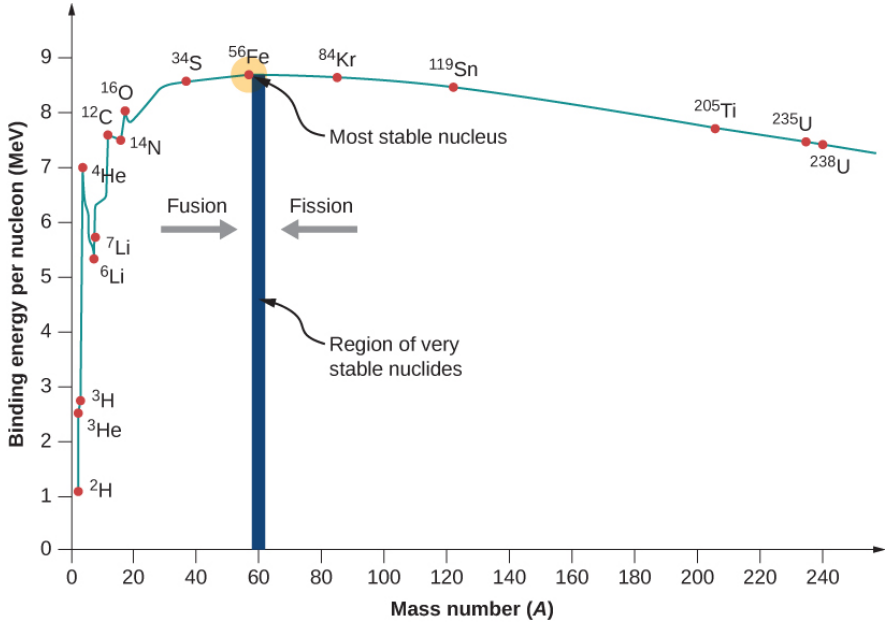

using a semi-empirical Weizsäcker formula, one can parameterize the binding energy in a liquid drop model

$$E_b(A) = A\left[15.8 - 18.3A^{-1/3} - 0.18A^{2/3} + 1.3\times10^{-3}A^{4/3} - 6.4\times10^{-6}A^{2}\right]$$

using energy conservation, one can calculate the energy required to separate a fragment F with N_F neutrons and Z_F protons

$$E_s = E_b(N,Z) - E_b(N_F,Z_F) - E_b(N-N_F,Z-Z_F)$$

This energy would be the threshold for the reaction $A \rightarrow F$ if the protons did not carry electric charge. The charge of the nucleus decreases E_s by an amount E_s^C, which represent the Coulomb barrier.

$$E_s^C \simeq \frac{Z_F(Z - Z_F)}{(A - F)^{1/3}}$$

the total energy needed to separate the fragment from the nucleus will be $E_s^{tot} = E_s - E_s^C$.

for heavy nuclei *(A>60)* an empirical distribution exists for the mass of the fragments

$$P(x) \propto 0.1/x^{2.5} + \exp(3.7x)$$

***x* ratio of fragment mass to mass of original nucleus**

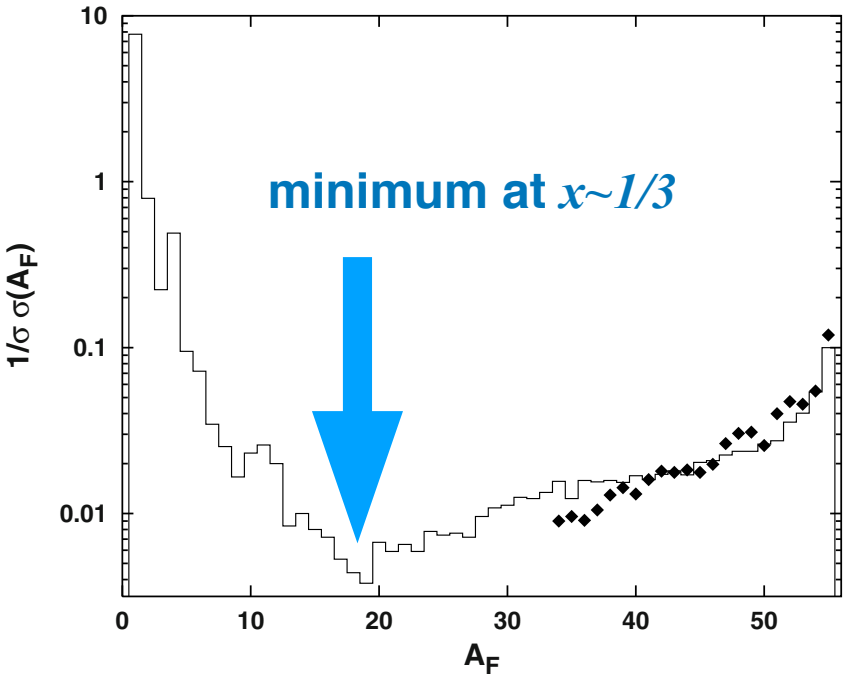

Fig. 2.10. Mass distribution of the fragments in Fe collisions on C target. The data are from Ref. [26] and the calculation is from Ref. [27].